Revista Geoaraguaia
ISSN:2236-9716
Barra do Garças – MT
v.10, n. esp. Geologia e
Pedologia p.33-55. Dez-2020

SEPARATING GEOCHEMICAL SEDIMENTS' ANOMALIES OF LITHIUM AND CONDUCTING STAGED FACTOR ANALYSIS BY THE USE OF CONCENTRATION-NUMBER FRACTAL MODELING ON SEDIMENTARY ROCKS OF THE JAM 1:100000 SHEET (NE IRAN)

SEPARAÇÃO DE SEDIMENTOS GEOQUÍMICOS ANÔMALOS DE LÍTIO E CONDUÇÃO DE ANÁLISE FATORIAL POR MEIO DO USO DA MODELAGEM FRACTAL DE CONCENTRAÇÃO-NÚMERO EM ROCHAS SEDIMENTARES DA FOLHA JAM 1: 100000 (NE IRÃ)

Leila Jaberansari[1]

Habiballah Torshizian*[2]

Nader Kohansal-Ghadimvand[3]

Mohsen Pourkermani[4]

ABSTRACT

Because of its special geochemical properties, lithium can be concentrated in sedimentary rocks. The current study was conducted on sedimentary units of the Jam 1:100000 sheet (NE Iran) by Concentration-Number(C-N) fractal models and staged factor analysis. Samples were based on stream sediment and lithogeochemical data. Concentration-Number fractal model was utilized to identify anomalous areas for lithium and the results were presented in the form of maps. According to the lithology of the area, which contains sedimentary units with various clay minerals, and the high correlation between lithium and three other elements (B, Rb, and Cs) in the anomalous area, an area in the southeast of Jam was found to contain the highest amount of lithium anomaly. This area should be further investigated in future studies. It is suggested that interested researchers use the two methods implemented in this study to explore lithium in sedimentary rocks and identify promising areas bearing lithium in Iran.

Keywords: Lithium; Geochemical exploration; Concentration-Number (C-N) fractal model; Staged factor analysis; Clay; Iran.

RESUMO

[1]Department of Geology, North Tehran Branch, Islamic Azad University, Tehran, Iran. leila_j55@yahoo.com ORCID: http://orcid.org/0000-0002-9181-4346

[2]Department of Geology, Mashhad Branch, Islamic Azad University, Mashhad, Iran. *Corresponding author email habib.torshizian@gmail.com ORCID: http://orcid.org/0000-0001-8662-8453

[3] Department of Geology, North Tehran Branch, Islamic Azad University, Tehran, Iran. nkohansal@yahoo.com ORCID: http://orcid.org/0000-0003-0706-5897

[4] Department of Geology, North Tehran Branch, Islamic Azad University, Tehran, Iran. mohsen.pourkermani@gmail.com ORCID: http://orcid.org/0000-0003-3445-760X

Devido às suas propriedades geoquímicas especiais, o lítio pode ser concentrado em rochas sedimentares. O presente estudo foi conduzido em unidades sedimentares da folha Jam 1: 100000 (NE Irã) por modelos fractal de Concentração-Número (C-N) e análise fatorial. As amostras foram baseadas em sedimentos de corrente e dados litoquímicos. O modelo fractal de número de concentração foi utilizado para identificar áreas anômalas de lítio e os resultados foram apresentados na forma de mapas. De acordo com a litologia da área, que contém unidades sedimentares com vários minerais argilosos, e a alta correlação entre o lítio e três outros elementos (B, Rb e Cs) na área anômala, foi encontrada uma área no sudeste de Jam que contêm a maior quantidade de amostras anômalas de lítio. Essa área deve ser investigada em estudos futuros. Sugere-se que os pesquisadores interessados usem os dois métodos implementados neste estudo para explorar o lítio em rochas sedimentares e identificar áreas promissoras com lítio no Irã.

Palavras-chave: Lítio; Exploração geoquímica; Modelo fractal de Concentração-Número (C-N); Análise fatorial; Argila; Irã.

INTRODUCTION

Due to their mineralogical and petrological properties, sedimentary units are lithium (Li) adsorbents. High dissolution of lithium in water and the abundance of sedimentary units such as clay, marl, and shale in the study area clearly demonstrate the significance of the study (Hadadan, 1994; Howard, 1981). Thus, upon studying various lithium exploration projects in different parts of the world – including lithium exploration from sedimentary rocks in Clayton Valley, Nevada – good information was obtained about the appropriate methodology, sampling, data analysis, and data interpretation (Carew 2016; Don 2016; Marvin 2017). Furthermore, in of Iran Azami (2012), Saadati (2012), Dabiri *et al.* (2018), Fyzollahhi *et al*. (2018), Nazarpour (2018), Yazdi *et al.* (2019 a&b) Yasrebi and Hezarkhani (2019) and Abdoli Sereshgi *et al*. (2019) were presented in the form of maps indicating anomalies in sedimentary rocks. At the end, because of the geological structure of Iran, lithium properties, and the superiority of fractal model to classic procedures in analyzing the data, the current study utilized Concentration-Number (C-N) fractal, which is a geochemical exploration method, by focusing on sedimentary rocks. Moreover, to gain better results, factor analysis was implemented as a practical technique and suitable model for lithium exploration.

Revista Geoaraguaia
ISSN:2236-9716
Barra do Garças – MT
v.10, n. esp. Geologia e
Pedologia p.33-55. Dez-2020

In geochemical exploration, areas with geochemical anomaly are identified since they are related to the mining of the study area, hence their identification is important in analyzing geochemical changes and the process of forming the mineral (Galuszka, 2007). In general, geochemical data have a multi-fractal behavior indicating geological, geochemical, alteration, and mining relations followed by the enrichment stages of an element (Cheng et al. 1994; Gonçalves *et al.,* 2001; Lima *et al.,* 2003; Afzal *et al*., 2010; Zuo, 2011; Nazemi *et al.,* 2019).

In geochemical exploration through fractal model, all data are utilized without any modification based on their structure and spatial location. Thus, geochemical anomalies are separated from their background in a much better way (Cheng *et al.,* 1994; Simmt and Davis, 1998; Davis, 2002; HassaniPak, 2005). In contrast, classic statistical procedures, which are based on some quantities like mean and standard deviation, cannot identify anomalies with high background values or weak anomalous values (Bai *et al.,* 2010; Hassanpour, Afzal, 2011; Baratian, 2018).

There are various fractal models to study earth sciences. These models were initially introduced by Mandelbrot (1983) and gradually used in identifying mineral areas, especially in geochemical explorations (Cheng *et al.,* 1994; Li *et al.,* 1994; Zuo, 2011). One of the most efficient fractal methods is the Concentration-Number (C-N) method, which was originally introduced by Hassanpour and Afzal (2011) and utilized in geochemical explorations of porphyry deposit in Haftcheshmeh, East Azerbaijan, Iran. On the other hand, staged factor analysis is useful in better identification of interdependent genetic relationships between different elements, exploration of available changes in geochemical environments, and categorization of data based on the indicators that are dependent on target deposit types (Yousefi *et al.*, 2014). Using factor analysis results in the reduction of the number of variables and makes it possible to identify the role of each factor in the variability (Van-Helvoort *et al.,* 2005; Afzal *et al.,* 2015).

This study aimed to introduce Concentration-Number (C-N) method for lithium exploration in Jam area and was presenting an extreme anomaly in its.

METHODOLOGY

CONCENTRATION-NUMBER FRACTAL MODEL

The Concentration-Number fractal model was first introduced by Hassanpour and Afzal (2011) based on Mandelbrot's (1983) Number-Size (N-S) model. This model indicates that there is a relationship between the elements' concentration and their cumulative number in the samples collected from a study area (Li *et al*., 1994) (Equation 1).

$$N(\geq \rho) = F\rho^{-D} \quad (1)$$

Where is the element's concentration, is the cumulative number of samples with concentrations bigger than or equal to, F is a constant, and D is the fractal dimension. According to Mandelbrot (1983) and Deng *et al.* (2010), the log-log plot of against illustrates pieces of direct lines with various slopes (-D) corresponding to different concentration intervals (Sadeghi *et al.*, 2012). A series of geochemical data comprises two connected fractal groups – namely the group representing the background and the one indicating anomaly.

To separate anomalous populations or statistical populations, attempts are made to consider critical concentrations (those intervals within which fractal dimension changes) as threshold values. Since fractal models establish exposure relations between these parameters, their diagram in the log-log plot will be manifested in the form of a direct line. Thus, the Concentration-Number diagram used in this study is illustrated in the form of two or more lines for exploratory data. The border between the two lines is a concentration indicating the threshold value. In fact, these two lines represent the background population and statistical population. They have two different slopes showing that their dimensions are different (Afzal *et al.*, 2015). In the current study, Excel Microsoft Office was used to complete all stages for processing geochemical data to separate statistical populations and draw the

log-log plot of the Concentration-Number fractal of lithium. The statistical populations were interpolated in the form of contour maps using Inverse Distance Weighted (IDW) procedure. Using this type of interpolation, the researchers divided the area into 350 m × 350 m cells in RockWorks 15.

STAGED FACTOR ANALYSIS

Staged factor analysis is suitable for analyzing geochemical data with numerous elements and can be utilized to identify major variables when the variance explained by each factor goes up. It can be used to show one or several geochemical anomalies (Afzal *et al.,* 2016). Since the elements that do not contribute to any factor are eliminated in staged factor analysis, multi-element anomalous areas can be obtained, which are essential to identify the type of mineralization of the study area (Rahimi *et al.,* 2017).

In the first phase of staged factor analysis, principal component analysis is conducted using varimax rotation with Kaiser normalization. The aim is to separate common factors. Then, Bartlett's test is carried out using factors with factor loadings greater than 1, which is important in determining the maximum number of factors in factor analysis (Davis 2002; Fyzollahi *et al,.* 2017). Examining the output of rotated component matrix will yield element or elements that are not loaded on any factor based on the determined threshold eigen value (less than 0.5). These elements are then excluded from the data (Fyzollahi *et al.,* 2017). This stage will continue until no unloaded element remains (Afzal *et al.*, 2015). *PSAW Statistics 18* (SPSS) was used in all processing phases of staged factor analysis.

GEOLOGICAL SETTING OF THE STUDY AREA

The study area is located in the Jam 1:100000 sheet, a region in the west of Semnan Province (NE Iran). The geological sheet of Jam is one of the six 1:250000 geological sheets of Semnan.

From the perspective of palegeography, Attari fault divides Jam into two zones – i.e. Alborz and Central Iran – with a northeast-southwest (NE-SW) trend (Alavi-Naini, 1972; Fotovati and Rezaeian, 2008) (Figure 1).

There is no evident geological difference between these two zones (Ghomayshi, 1997). However, the effects of plate tectonics and sedimentary basins within the fault zone have led to some changes in the lithology and the thickness of stratigraphic units with the same age (Fotovati and Rezaeian, 2008). The most important sediment formations of the Jam are Soltaniyeh, Mobarak, Shemshak, Karaj, Lower red, Qom and Upper red. These stratigraphic series entail 12000 m thick units whose age ranges from Cambrian to quaternary. The igneous rocks of the area are mostly acid tuff, dacite, rhyolite, silicic igneous rocks, andesite, and some mafic igneous rocks. Intrusive rocks do not have significant outcrop in the study area. There are a lot of sedimentary units in the sheet of Jam, which includes clay minerals, e.g. shale, marl of Shemshak formation, (they are as old as the quaternary) (Ghomayshi, 1997) (Figures 2 and 3).

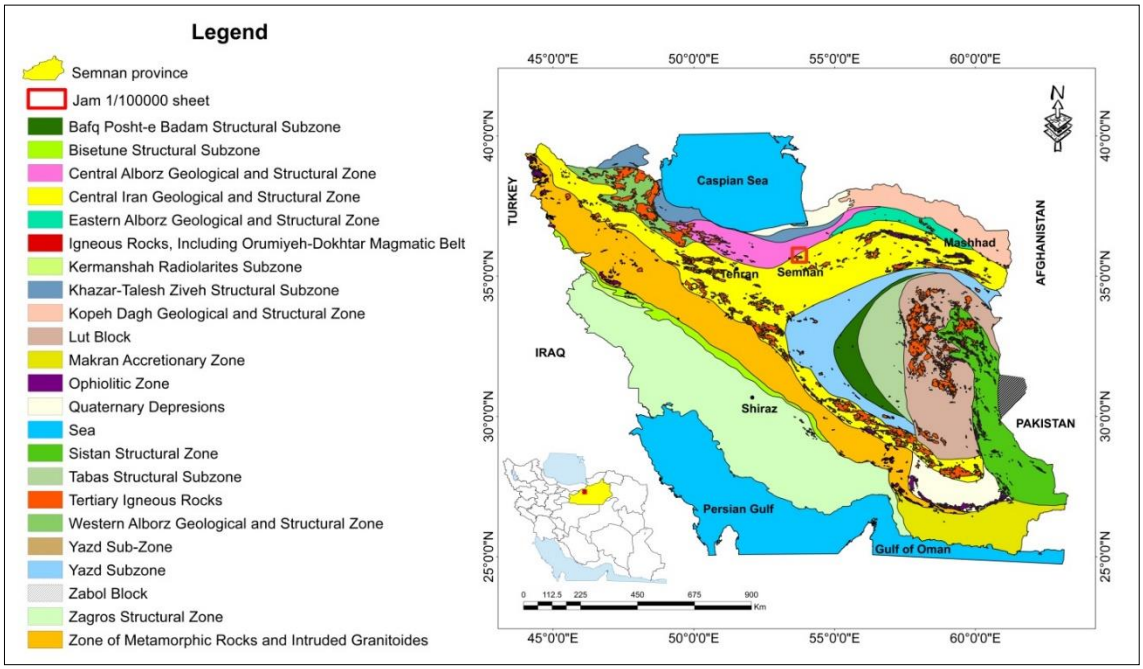

Figure 1. The location of the Jam 1:100000 sheet in structural map of Iran.
Source: Aghanabati (2004).

The most important faults in the study area are Attari, Peyghambaran, Namaard, Naeek, Jan, Masoumzadeh, and Louver. The trend in all of them is NE-SW (Alavi-Naini, 1972; Ghomayshi, 1997).

With respect to mineralization, Jam is located within the iron mineralization belt of Semnan, which begins from the north of Semnan and stretches to the southeast of Shahrud (Haji Bahrami *et al.*, 2016). Sheykhaab, Hamirod, Ajat -Abad, and Jam are some of the iron deposits in the area. They have been developed out of vein hematite, which in turn has been formed through the permeation of intrusive igneous rocks in limestone and pyroclastic sedimentary rocks of Karaj formation (which is as old as the middle Eocene) or cretaceous limestone (Fotovati and Rezaeian, 2008).

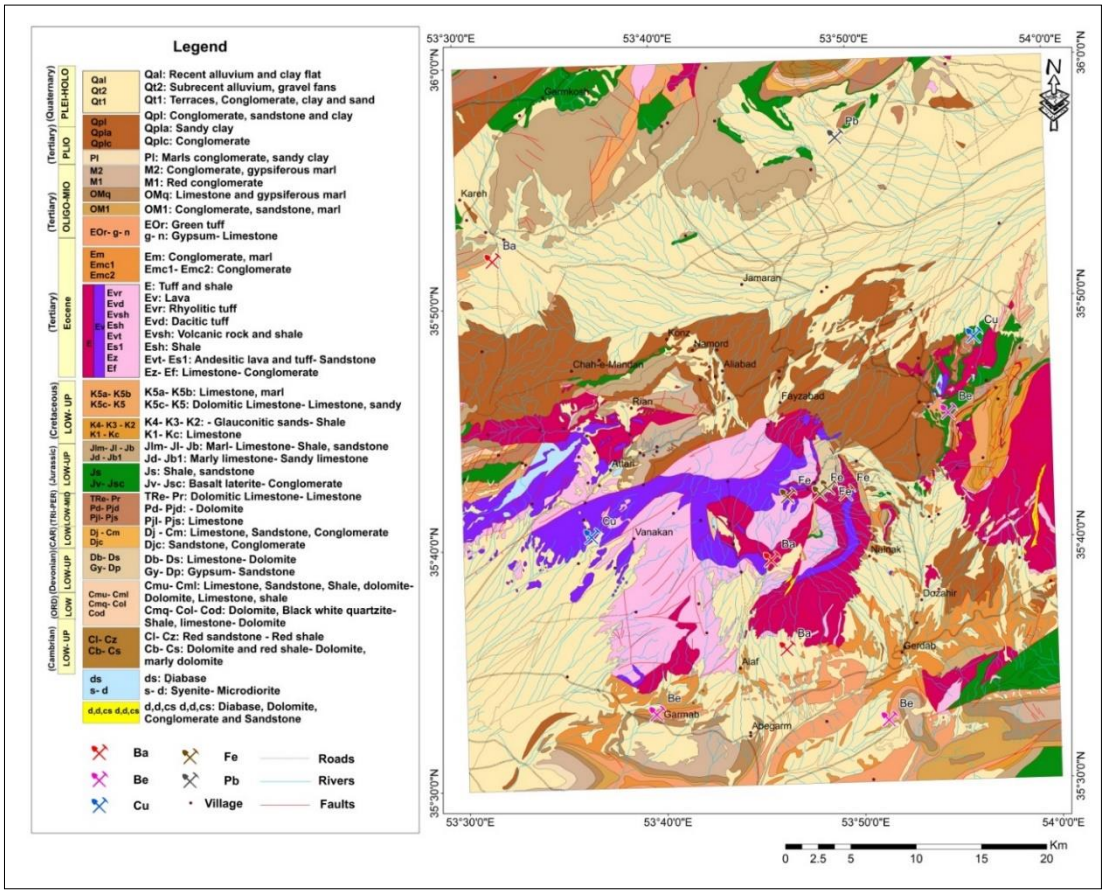

Figure 2. The simplified geological map of the Jam 1:100000 sheet.
Source: Ghomayshi (1997).

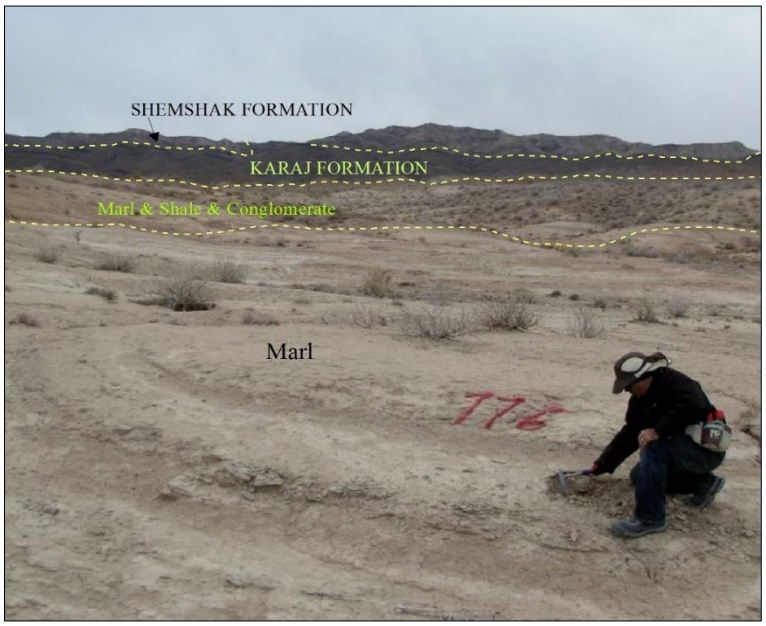

Figure 3. The most important geological formations of the Jam 1:100000 sheet.
Source: Authors (2020).

DISCUSSION

GEOCHEMICAL DATA

1. Stream sediment samples

First stage, the data related to 1009 stream sediment samples which had been collected by Jiangxi Company (1999) from the entire Jam 1:100000 sheet – were used. The distance between stream sediment samples was 1400 m, their weight was between 400 and 500 g, and their size was -40 mesh. The 29 element analysis of samples was carried out for lithium using ICP with the detection limit of 1 ppm (Jiangxi, 1996) (Figure 4a).

2. Lithogeochemical samples

Second stage, 42 lithogeochemical samples were collected from the identified anomalous area, which comprised 3 study blocks. Chip channel method was used for collecting samples that were 3 kg and were 500 m apart from each other. These samples were chemically analyzed for lithium using flame photometer with the detection limit of 5 ppm in Geological survey and mineral exploration of Iran (Figure 4b-c).

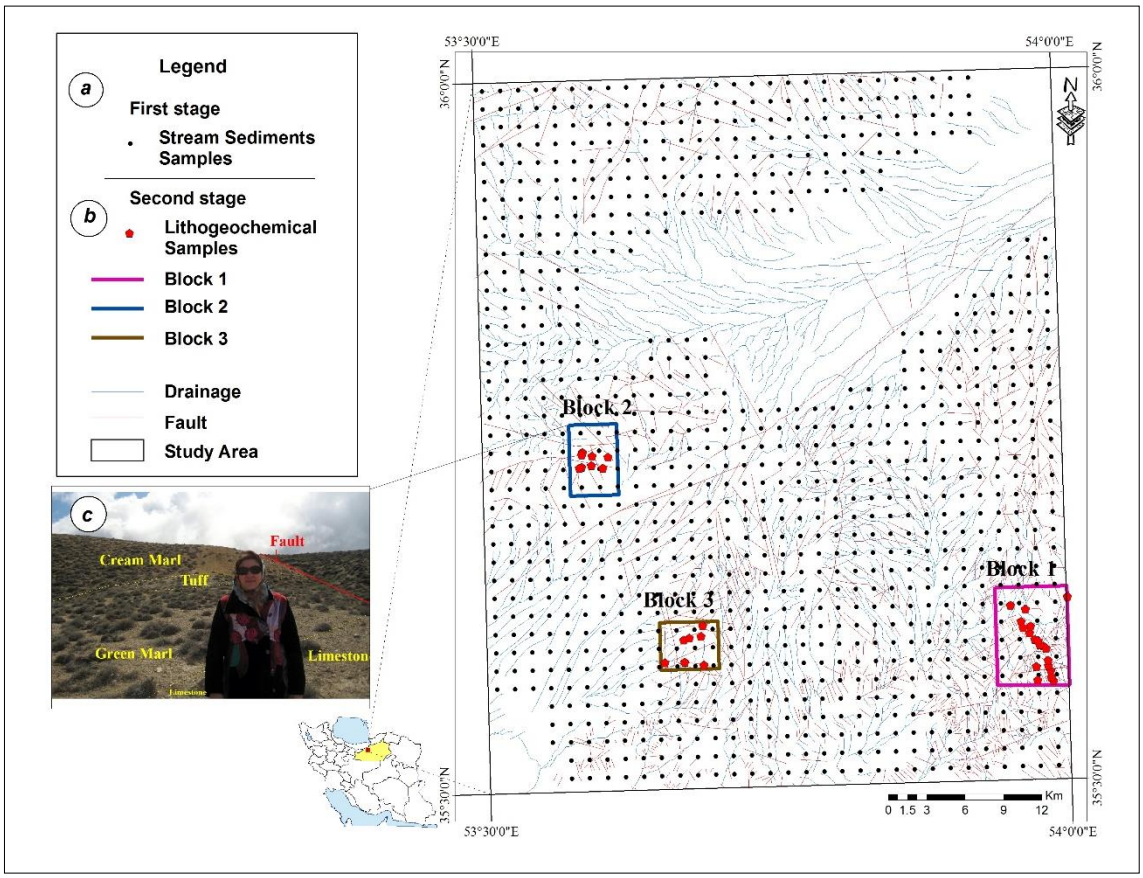

Figure 4. The sampling location map of the Jam 1:100000 sheet; (*a*) stream sediment data; (*b*) lithogeochemical data samples; (*c*) Lithogeochemical samples were collected from the identified anomalous area by student.
Source: Authors (2020).

Through drawing the cumulative histogram of lithium for the stream sediment samples, the ore grades that did not belong to any category were identified. It was not logical to eliminate these ore grades, especially the high ore grades, because anomalous areas would be deleted. Thus, Doerffel method was used to replace the out of category grades with appropriate values with a 99% confidence interval (Hawkes and Webb, 1962; Barak *et al.,* 2017) (Figure 5).

Furthermore, the cumulative histogram of lithium was drawn for the lithogeochemical samples based on these values that were not out of category (Figure 5).

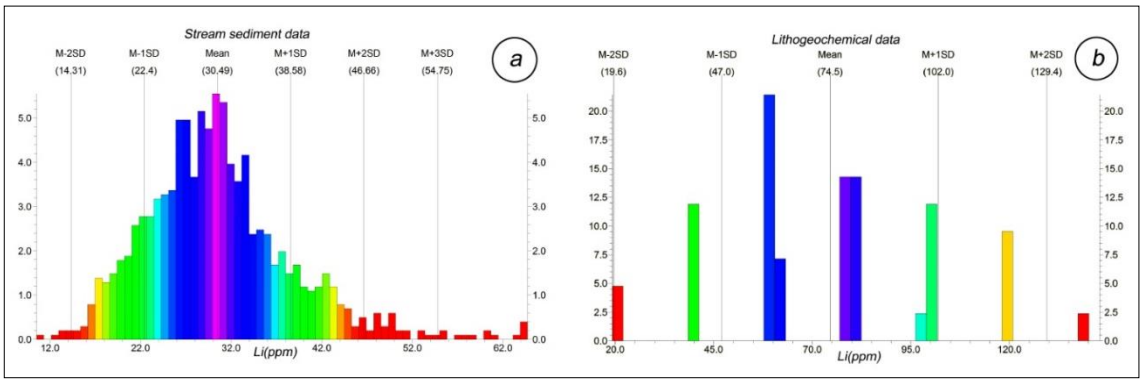

Figure 5. The histogram of lithium; (*a*) stream sediment data; (*b*) lithogeochemical data.
Source: Authors (2020).

On the average, the amounts of lithium in stream sediments and lithogeochemical samples respectively were 30.49 ppm and 74.5 ppm. Moreover, the maximum amounts were 64.9 and 138.26 ppm (Table 1). These values obtained through conducting geochemical analysis are bigger than the average amount of lithium in the earth crust (17-20 ppm) (Kunasz, 2006; Evans, 2014), indicating the concentration of lithium in the study area. Rock Works 15 was used to draw histograms and conduct statistical parameters of lithium.

Stream sediment		**Lithogeochemical data**	
Statistical parameters	Li(ppm)	Statistical Parameters	Li(ppm)
Mean	30.54	Mean	74.50
Std. Deviation	8.34	Std. Deviation	27.48
Variance	69.48	Variance	754.72
Minimum	10.71	Minimum	19.63
Maximum	85.73	Maximum	138.26
Skewness	1.26	Skewness	0.179
Kurtosis	4.27	Kurtosis	-0.43

Table 1. Statistical arameters calculated for lithium based on stream sediment data and lithogeochemical data.
Source: Authors (2020).

APPLICATION OF STAGED FACTOR ANALYSIS

Three rounds of factor analysis were conducted on stream sediment data to extract the major factors in relationship with lithium mineralization.This operation was carried out in three stage. Six factors (Ba,W, Th, Ni, Au, U) have been removed from rotated factor matrix for the three staged factor analyses because elements are less than 0.5 scores. Factor scores $\geq$ 0.5 were used in this study because they have high correlation with each others.

As a result in third rotated factor matrix, the number of elements was reduced from 29 to 23. The results of factor analysis of elements like Cs, Rb, B, and Li (known as F2-3) show that these elements are highly correlated, with the highest value belonging to factor 2 in stage 3. Lithium paragenesis was separated out by taking F2-3. This factor was used for C-N modeling of Li anomalous parts in the Jam area (Table 2).

First stage	**Rotated Component Matrix(1)**						
	Component						
	1	**2**	**3**	**4**	**5**	**6**	**7**
Li	.276	.786*	.047	-.001	.055	-.032	.224
Na2o	.636	-.137	.134	.230	.077	.002	.495
Zn	.385	-.014	.037	.161	.031	.815	-.097
Pb	.122	-.099	.194	.018	.024	.891	.003
Ag	.047	-.032	.314	.566	.056	.436	.177
Cr	.590	.540*	-.135	.120	-.220	.166	-.198
Ni	.528	.524*	.006	-.216	-.127	.174	-.248
Bi	.234	.183	.565	.111	.432	-.140	-.184
Cu	.750	.133	.154	.060	.263	.145	.160
As	.038	.161	.743	-.210	.217	.141	-.052
Sb	.193	-.144	.771	.329	.156	.116	.025
Co	.862	.084	.326	.081	.101	.095	-.016
Sn	.506	.361	.021	.187	.363	.250	-.011
*Ba***	.329	-.348	.466	.179	.206	-.204	.269
V	.751	.118	.197	.478	.086	.153	.069
Sr	-.091	.030	-.107	.004	.012	-.076	.896
Hg	.142	.199	.704	.107	-.087	.203	.010
*W***	.423	.378	.256	.080	.484	-.216	-.285
B	-.125	.809*	.037	.022	.172	-.159	.036
Be	.656	.327	.097	.289	.412	.234	-.069
Mo	.235	-.139	.110	.218	.446	.105	.596
Au	.340	.067	.162	-.089	.512	-.083	.103
Rb	.220	.725*	.158	.291	.373	-.046	-.169

P	.357	.101	-.010	.818	.011	.046	.043
Cs	.037	.779*	.138	.234	.196	.017	-.174
Nb	.798	-.079	.096	.113	.388	.174	-.095
*Th***	.299	.143	.170	.110	.498	.241	.072
U	.007	.304	.063	.224	.637	.023	.188
F	.093	.378	.101	.780	.308	.027	.051

Rotated Component Matrix(2)							
	Component						
Second stage	**1**	**2**	**3**	**4**	**5**	**6**	**7**
Li	.273	.764*	-.007	-.038	-.002	.143	
Na2o	.660	-.149	.034	.216	.036	.433	
Zn	.386	.003	.039	.144	.809	-.089	
Pb	.123	-.090	.179	.009	.892	.017	
Ag	.066	-.009	.268	.541	.487	.214	
Cr	.521	.491	-.236	.077	.230	-.338	
*Ni***	.468	.497	-.059	-.255	.228	-.357	
Bi	.302	.236	.672	.144	-.180	-.059	
Cu	.783	.176	.156	.038	.154	.176	
As	.084	.149	.785	-.196	.133	.015	
Sb	.226	-.133	.734	.341	.159	.064	
Co	.864	.085	.270	.068	.130	-.068	
Sn	.568	.420	.125	.176	.188	.071	
V	.767	.120	.142	.463	.175	.025	
Sr	-.074	.024	-.225	-.034	-.024	.831	
Hg	.138	.130	.615	.099	.255	-.052	
B	-.125	.838*	.051	-.001	-.131	.050	
Be	.719	.400	.194	.287	.175	.011	
Mo	.329	-.051	.166	.204	.087	.727	
*Au***	.439	.149	.322	-.079	-.170	.256	
Rb	.261	.785*	.247	.292	-.077	-.095	
P	.358	.116	-.069	.802	.087	.026	
Cs	.043	.810*	.175	.220	.031	-.140	
Nb	.858	-.012	.190	.129	.111	-.011	
*U***	.132	.431	.267	.229	-.085	.394	
F	.149	.443	.155	.777	.011	.142	

Rotated Component Matrix(3)
Component

Third stage	1	2	3	4	5	6	7
Li	.291	.799*	.006	-.108	.022	.162	
Na2o	.673	-.104	.046	.144	.036	.471	
Zn	.404	-.001	.033	.152	.820	-.099	
Pb	.132	-.090	.185	.040	.901	.013	
Ag	.058	-.033	.274	.644	.425	.214	
Cr	.508	.471	-.222	.096	.213	-.292	
Bi	.315	.233	.676	.146	-.221	-.070	
Cu	.764	.136	.177	.088	.109	.187	
As	.074	.144	.794	-.160	.125	-.002	
Sb	.231	-.144	.747	.380	.098	.071	
Co	.864	.073	.292	.052	.095	-.027	
Sn	.585	.421	.106	.161	.200	.032	
V	.790	.131	.138	.421	.152	.039	
Sr	-.094	.046	-.171	-.006	-.062	.891	
Hg	.156	.156	.630	.064	.250	-.022	
B	-.126	.836*	.062	.020	-.143	.048	
Be	.747	.387	.179	.260	.165	-.022	
Mo	.332	-.077	.185	.246	.034	.704	
Rb	.286	.789*	.230	.269	-.081	-.126	
P	.388	.115	-.088	.787	.047	.022	
Cs	.054	.819*	.167	.223	.031	-.152	
Nb	.884	-.012	.167	.071	.125	-.046	
F	.189	.444	.129	.767	-.023	.100	

*Bold numbers represent the selected factors based on the threshold of 0.5
**Bold elements represent have been removed from stages

Table 2. The rotated factor matrix for the three staged factor analyses.
Source: Authors (2020).

APPLICATION OF CONCENTRATION-NUMBER FRACTAL MODEL

Upon determining the threshold values and separating geochemical anomalies from the background, the data (for lithium and factor structures) were ordered from the highest to the lowest. Then, Concentration-Number analysis was conducted to determine their frequency. The log-log plots of cumulative frequency of lithium number against its concentration and cumulative frequency of components (Cs, Rb, B, and Li) number against its concentration were depicted. The log-log plots were generated for separation of lithium anomalies in sediment (Figure 6).

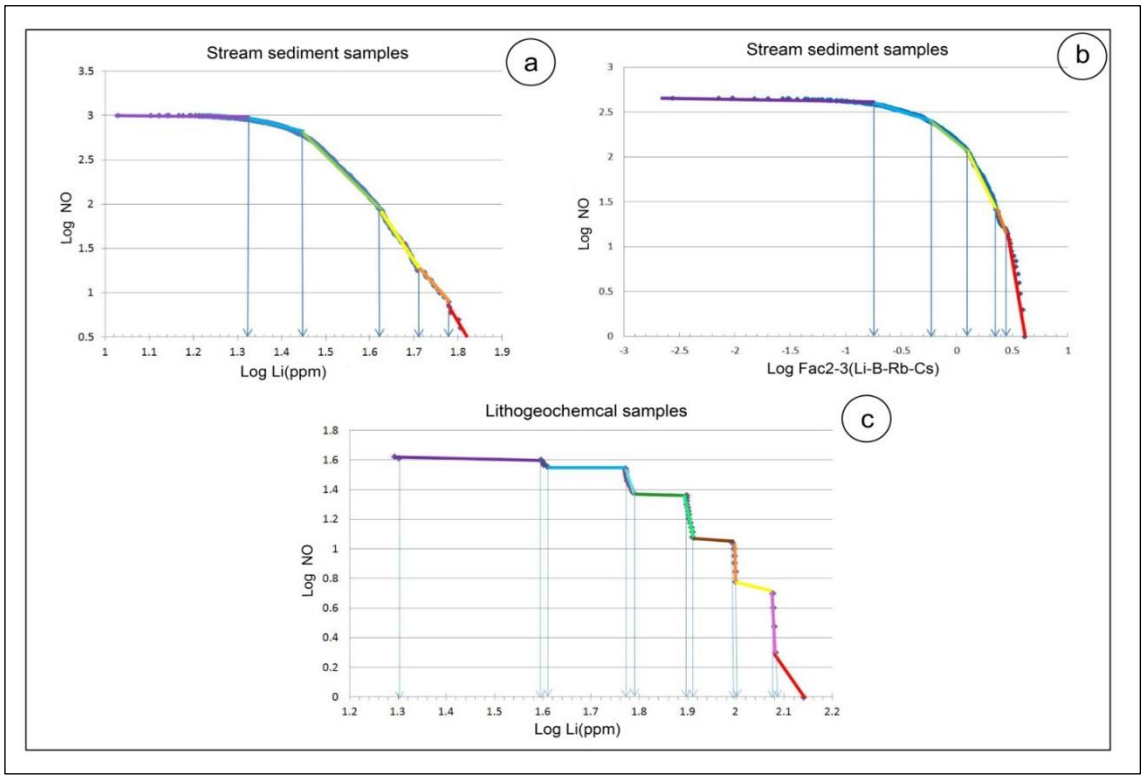

Figure 6. (*a*) C-N log-log plots for lithium based on stream sediment samples; (*b*) C-N log-log plots for factor analysis F2-3 (Li-B-Rb-CS) based on stream sediment samples; (*c*) C-N log-log plots for lithium based on lithogeochemcal samples.
Source: Authors (2020).

The direct lines were then analyzed to obtain a series of points through calculating the breakpoints. As a result, the statistical populations for lithium and its factorial component structure were determined. In the stream sediment samples, the results of C-N analysis of lithium yielded six statistical populations. The first statistical population includes values smaller than 20 ppm. For lithium, these values are equal to those of the background. The second population entails values ranging from 20 ppm to 28 ppm, which indicate the weakly anomaly for lithium. The third population involves values varying from 28 ppm to 41 ppm, demonstrating the medium anomaly for lithium. The fourth statistical population encompasses values ranging from 41 ppm to 51 ppm, hence the medium anomaly for lithium. The fifth statistical population includes values ranging from 51 ppm to 60 ppm, showing the

high anomaly for lithium. The sixth population includes values ranging from 60 ppm to 63.9 ppm and values larger than this range the extreme anomaly for lithium (Table 3).

This last population illustrates the fifth anomaly for lithium and is located in a region in the southeast of the study area, which is separated from other anomalous areas in the map using red (Figure 7a).

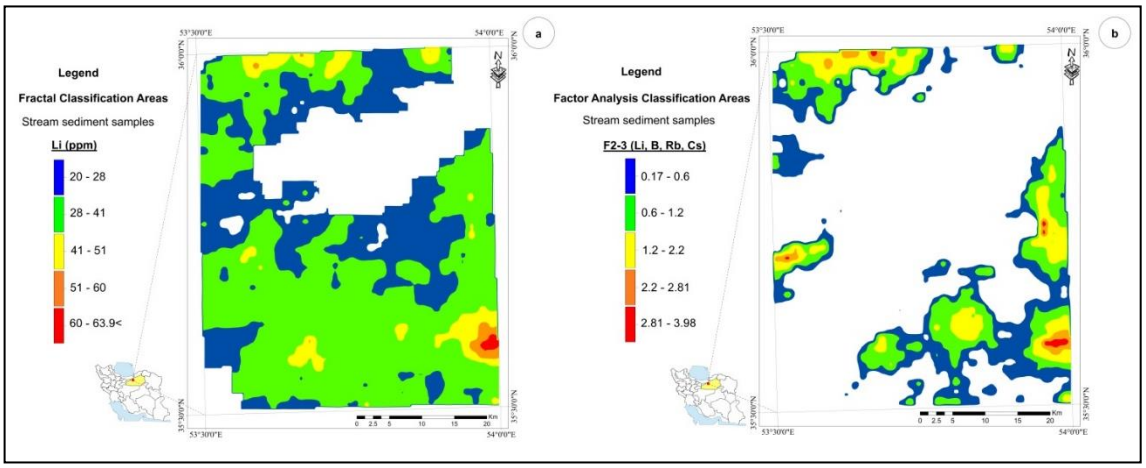

Figure 7. (*a*) Geochemical distribution map of lithium based on stream sediment samples by C-N fractal model in the Jam 1:100000 sheet; (*b*) Factor analysis F2-3 (Li-B-Rb-Cs) map based on stream sediment samples by C-N fractal model in the Jam 1:100000 sheet.
Source: Authors (2020).

On the other hand, the factorial component structure (F2-3) of C-N method, including Li, Rb, B, and Cs, yielded six statistical populations (Table 3). The sixth statistical population, which contains the highest values (F2-3=2.81-3.98) and the extreme anomaly for Cs, Rb, B, and Li, indicates the concentration of the above-mentioned elements (Lithium paragenesis) in a vast territory in the east and southeastern part of the study sheet and a small part in the northern and wes Moreover, the statistical populations calculated through C-N model of lithium in the lithogeological samples were divided into seven populations (Table 3). The first population included values smaller than 19.6 ppm, which is equal to the background values for lithium. The second population encompassed values ranging from 19.6 ppm to 40 ppm, indicating the weakly anomaly samples of lithium. The third population entailed values ranging from 40 ppm to 63 ppm, hence the weakly anomaly for lithium. The

fourth population covered values varying from 63 ppm to 79.4 ppm, demonstrating the medium anomaly samples for lithium. The fifth population encompassed values ranging from 79.4 ppm to 100 ppm, representing the medium anomaly for lithium. The sixth population included values ranging from 100 ppm to 120.2 ppm, hence the high anomaly for lithium. The seventh statistical population included values ranging from 120.2 ppm to 138.26 ppm as well as larger values. This population represents the extreme anomaly for lithium in the lithogeochemical samples. These anomalous samples were in the southeast of Jam sheet and are represented using red (Figure 8) area of Jam sheet (Figure 7b).

Figure 8. Lithogeochemical distribution map of lithium by C-N fractal model in the Jam 1:100000 sheet. Source: Authors (2020).

Stream Sediment Sample							
Element	**The First population**	**The Second populat**	**The Third populati**	**The Fourth populati**	**The Fifth population**	**The Sixth populati**	**The Seventh population**
Level c anomal							**xtreme nomaly**
Li (ppn							-
F2-3 (Li,B,Rb,							-
Li (ppn							138.26

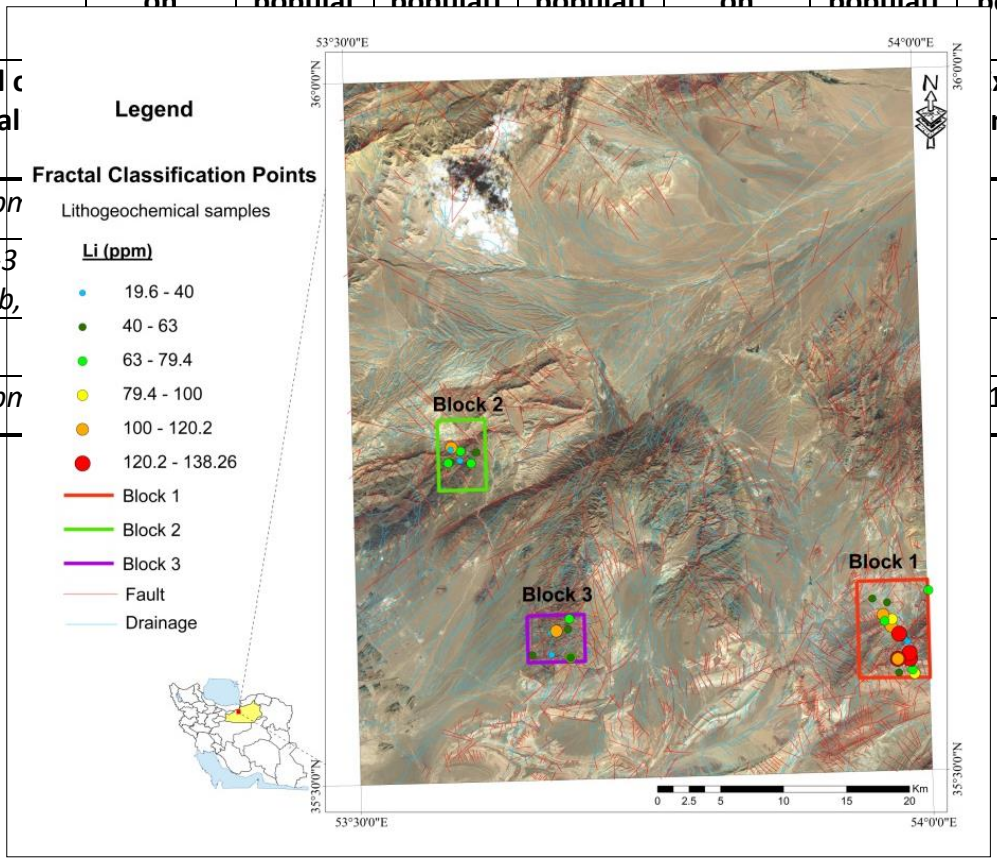

Table 3. Populations obtained by C-N fractal model based on stream sediment samples and lithogeochemical samples.

Source: Authors (2020).

EXAMINING THE OVERLAP BETWEEN STREAM SEDIMENT SAMPLES AND LITHOGEOCHEMICAL SAMPLES

In order to examine the validity of obtained anomalies, lithogeochemical samples were collected from suitable lithology located in the anomalous samples of stream sediments. Overlapping maps in both stages indicated that block 1 has the biggest amount of lithium samples (Li≥120.2 ppm). The areas with average or severe anomaly are represented using orange and red in the map (Figure 9a). Furthermore, overlapping the maps of staged factor analysis and lithogeochemical samples indicated that lithogeochemical samples (with Li values' greater than 120.2 ppm) are located in areas where the correlation between Li, Rb, B, and Cs is high (Figure 9b).

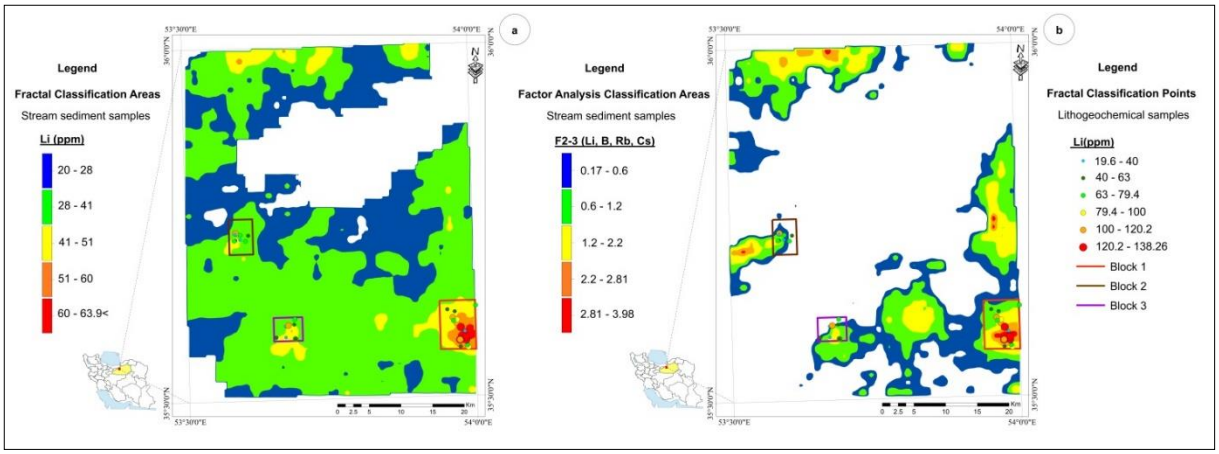

Figure 9. (*a*) Overlap between geochemical and lithogeochemical distribution map of lithium by C-N fractal model in the Jam 1:100000 sheet; (*b*) Overlap between factor analysis F2-3 (Li-B-Rb-Cs) and lithogeochemical distribution map of lithium by C-N fractal model in the Jam 1:100000 sheet.
Source: Authors (2020).

EXAMINING THE OVERLAP BETWEEN GEOCHEMICAL STUDIES AND THE LITHOLOGY OF THE AREA

Examining the overlap between lithogeochemical samples where the amount of lithium is greater than 100 ppm and simplified geological maps of Jam shows that the geological units of block 1 (which cover an area of about 3.77 square kilometer) have the

highest mineralization potential in rock units, limestone, marl, clay, shale, sandstone, and dacitic tuff. Field observation and petrological studies of rocks in the study area confirm the correlation between lithology and the amount of lithium. On the other hand, rhyolite units and acid tuff are highly important in this region since they are the origin of lithium (Brown, 2016; Benson *et al.*, 2017) (Figure 10).

In addition, the highest amount of lithium (Li = 138.26 ppm) in block 1 was obtained from Shemshak formation and comprised rock units containing sandstone, shale, thin layers of limestone as old as the Jurassic period (Figure 9). Normally, shale contains clay minerals like illite (Howard, 1981; Grim, 1953). According to Norouzi (2017) and Abedini (2017), the shale of Shemshak formation contains illite, which is capable of absorbing lithium (Klein *et al.,* 1999). Thus, the shale layers in the region contain the highest amount of lithium.

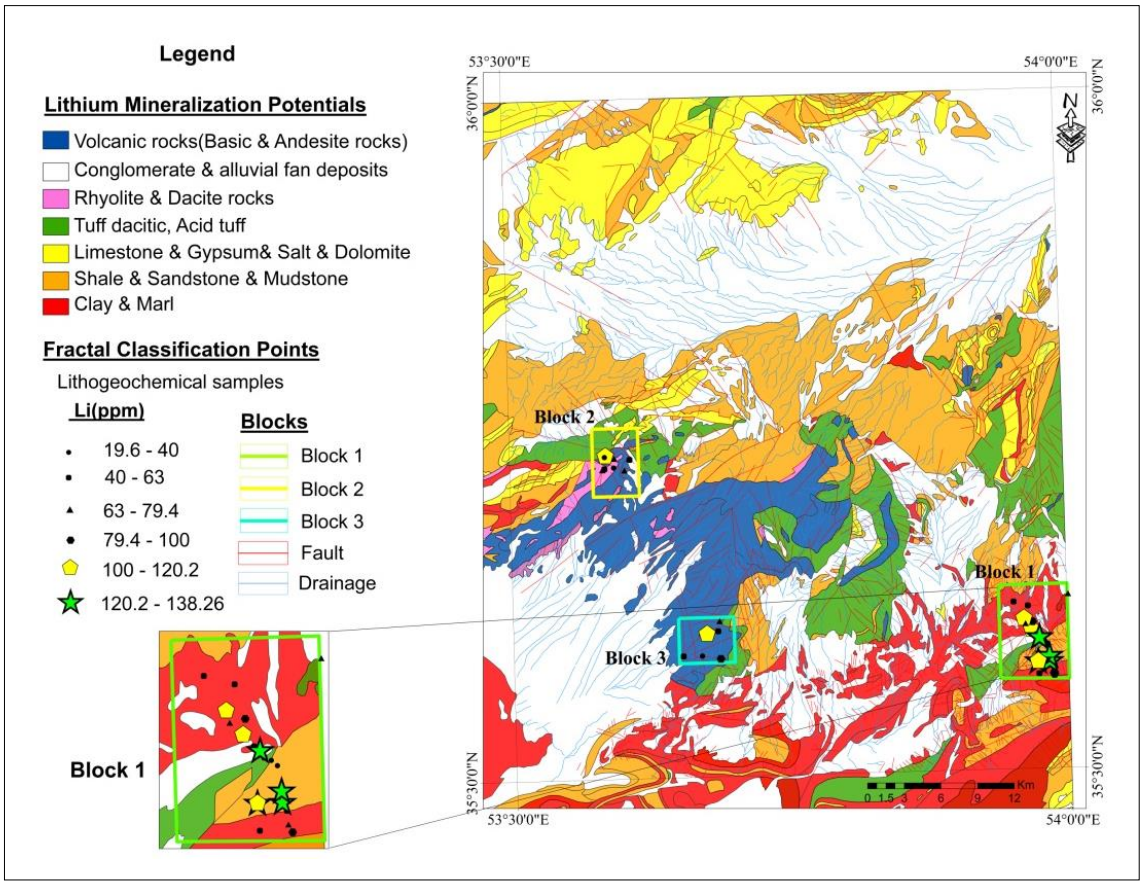

Figure 10. The overlap between the simplified geological map with anomalous samples that contain the highest amounts of lithium.
Source: Authors (2020).

Revista Geoaraguaia
ISSN:2236-9716
Barra do Garças – MT
v.10, n. esp. Geologia e
Pedologia p.33-55. Dez-2020

CONCLUSION

Concentration-Number fractal model and staged factor analysis were the two procedures used in this study. The anomalous area for lithium can be identified using this procedure. The combination of C-N fractal model and staged factor analysis techniques were identificated of anomalous areas where lithium can be found. Analysis was care on the stream sediment data and it's result show that lithium and it's paragenesis exist in F2-3. Anomalous areas were checking by lithogeochemical samples. The amount of lithium is determined based on the degree of paragenetic elements with high correlations that are located in a single factor and had the highest concentration in a particular area. The overlap between the findings of the two procedures revealed that the most anomalous area for lithium is located in the southeastern part of the Jam sheet.

The results indicated that the major anomaly in the southeastern part of Jam sheet is located in block 1 with (Li = 138.26 ppm) and has a lithology comprising clay and shale. It also contains clay minerals. Furthermore, in this block, lithium has the highest correlation with its paragenetic elements (B, Rb, and Cs). This study shows that the abovementioned methods are useful for studying sedimentary rocks and generalizing the findings to other area. Further studies are required to gain better understanding of minerals in various area.

ACKNOWLEDGEMENT

The researchers are grateful to Iranian Mines and Mining Industries Development and Renovation Organization (IMIDRO) for sponsoring this project.

REFERENCES

ABDOLI SERESHGI, H.; GANJI, A.; ASHJA ARDALAN, A.; TORSHIZIAN, H.; TAHERI, J.; Detection of metallic prospects using staged factor and fractal analysis in Zouzan region, NE Iran, **Iranian Journal of Earth Sciences**, 11(4), 2019. p.256-266.

ABEDINI, A.; Geochemistry of shales of the Shemshak formation of the Dash-Aghel mining district, Bukan, NW Iran: Provenance, source weathering, paleo-oxidation conditions, and tectonic setting. **Journal of Sedimentary Facies**, 9, 2017. p.53-72.

AFZAL, P.; KHAKZAD, A.; MOAREFVAND, P.; OMRAN, N. R.; ESFANDIARI B.; ALGHALANDIS, Y. F.; Geochemical anomaly separation by multifractal modeling in Kahang (Gor Gor) porphyry system, Central Iran. **Journal of Geochemical Exploration**, 104, 2010. p.34-46.

AFZAL, P.; MIRZAEI, M.; YOUSEFI, M.; ADIB, A.; KHALAJMASOUMI, M.; ZIA ZARIFI, A.; FOSTER, P.; YASREBI, A.; Delineation of geochemical anomalies based on stream sediment data utilizing fractal modeling and staged factor analysis. **Journal of African Earth Sciences**, 119, 2016. p.139-149.

AFZAL, P.; REZAEI, S.; LOTFI, M.; JAFARI, M.R.; MEIGONY, M. S.; KHALAJMASOUMI, M.; (2015) Investigation of copper and gold prospects using index overlay integration method and multifractal modeling in Saveh 1:100,000 sheet, Central Iran. **Gospodarka Surowcami Mineralnymi**, 31, 2015. p.51-74 .

AGHANABATI, S. A.; **Geology of Iran**. Geological Survey of Iran: Tehran, 2004.

AGTERBERG, F. P.; Multifractal Modeling of the Sizes and Grades of Giant and Supergiant Deposits. **International Geology Review**, 37, 1995. p.1-8.

ALAVI-NAINI, M.; Etude geologique de la region de Djam. **Geological Report 23**, Geological Survey of Iran: Tehran, 1972.

AZAMI, H.; Mineral Exploration Plan in Khorasan Razavi Provinces, South, North; Exploration of Li element in parts of Khorasan Razavi province. G**eological Report,** Geological Survey of Iran: Tehran, 2012.

BAI, J.; PORWAL, A.; HART, C.; FORD, A.; YU, L.; Mapping geochemical singularity using multifractal analysis: Application to anomaly definition on stream sediments data from Funin Sheet, Yunnan, China**. Journal of Geochemical Exploration**, 104, 2010. p.1-11.

BARAK, S.; BAHROUDI, A.; JOZANIKOHAN, G.; Exploration of neysian area by geochemical data and fractal concentration-number (C-N). **National Conference on Science Engineering**, 2010, p.1-10.

BARATIAN, M.; ARIAN, M. A.; YAZDI, A.; Petrology and petrogenesis of the Siah Kuh intrusive Massive in the South of Khosh Yeilagh. **Amazonia Investiga**, 7(7), 2018. p. 616-629.

BENSON, T.; COBLE, M. A.; RYTUBA, J. J.; MAHOOD, G.; (2017) Lithium enrichment in intracontinental rhyolite magmas leads to Li deposits in caldera basins. **Nature Communications**, 8, 2017. p. 270. <https://www.nature.com/articles/s41467-017-00234-y>

BROWN, T.; WALTERS, A.; IDOINE, N.; GUNN, G.; SHAW, R. A.; RAYNER, D.; **Lithium**. British Geological Survey: Nottingham, UK, 2016.

CAREW, T.; GEO, J. P.; ROSSI, M. E.; **Independent Technical Report for the Lithium** Nevada project, Nevada, USA. SRK Consulting (Canada) Inc: 19, 2016.

CHENG, Q.; AGTERBERG, F. P.; BALLANTYNE, S. B.; (1994) The separation of geochemical anomalies from background by fractal methods. **Journal of Geochemical Exploration** 51(2), 1994. p.109-130. <https://www.sciencedirect.com/science/article/pii/ 0375674294900132>

DABIRI, R.; AKBARI-MOGADDAM, M.; GHAFFARI, M.; Geochemical evolution and petrogenesis of the eocene Kashmar granitoid rocks, NE Iran: implications for fractional crystallization and crustal contamination processes. **Iranian Journal of Earth Sciences**, 10(1), 2018. p. 68-77.

DAVIS, J. C.; **Statistics and data analysis in geology**, 3 rd edn, Wiley: New York, 2002.

DENG, J.; WANG, Q.; YANG, L.; WANG, Y.; GONG, Q.; LIU, H.; Delineation and explanation of geochemical anomalies using fractal models in the Heqing area, Yunnan Province, China. **Journal of Geochemical Exploration,** 105, 2010. p. 95-105.

DON, M.; **Lithium Brine/Claystone Company Advancing Projects in Nevada**, Clayton Valley Project. Cypress Development Corp., 2016. p. 1-22. <https://www.slideshare.net/Companyspotlight/cypress-development-corp-investor-presentation>

EVANS, K.; **Lithium, Critical Metals Handbook**. American Geophysical Union, 2014. p. 230-261.

FOTOVATI, V. O.; REZAEIAN, Z. M.; **Mineral Reservoir 1: 250,000 sheets in Semnan Province**. Geological Report, Geomax Management of Geological Survey of Iran: Tehran, 2008.

FYZOLLAHHI, N.; TORSHIZIAN, H.; AFZAL, P.; JAFARI, M. R.; Determination of lithium prospects using fractal modeling and staged factor analysis in Torud region, NE Iran. **Journal of Geochemical Exploration**, 189, 2018. p.2–10.

GAŁUSZKA, A.; A review of geochemical background concepts and an example using data from Poland. **Environmental Geology**, 52, 2007. p. 861-870.

GHOMAYSHI, A.; **Geological Map of 1/100000 Jam**. Geological Survey of Iran: Tehran, 1997.

GONÇALVES, M. A.; MATEUS, A.; OLIVEIRA, V.; Geochemical anomaly separation by multifractal modeling. **Journal of Geochemical Exploration**, 72, 2001. p. 91-114.

GRIM, R. E.; **Clay mineralogy**. Mcgraw-Hill Book Company: New York, 1953.

HADADAN, M.; **Geological Map of 1/250000 Semnan**. Geological Survey of Iran: Tehran, 1994.

HASSANIPAK, A. A.; **Data analysis of exploration**. Tehran University publisher: Tehran, 2005.

HASSANPOUR, S.; AFZAL, P.; Application of concentration–number (C–N) multifractal modeling for geochemical anomaly separation in Haftcheshmeh porphyry system, NW Iran. **Arabian Journal of Geosciences**, 6, 2011. p.957-970.

HAWKES, H.E.; WEBB, J. S.; **Geochemistry in mineral exploration by H.E. Hawkes and J.S. Webb**. Harper & Row: New York, 1962.

HORSTMAN, E. L.; The distribution of Lithium, rubidium and caesium in igneous and sedimentary rocks**. Geochimica et Cosmochimica** Acta 12, 1957. p. 1-28.

HOWARD, J. J. Lithium and Potassium Saturation of Illite/Smectite Clays from Interlaminated Shales and Sandstones. **Clays and Clay Minerals**, 29, 1981. p. 136-142. <https://www.researchgate.net/publication/249899033>.

KLEIN, C.; HURLBUT, C. S.; DANA, J. D. **Manual of Mineralogy**. John Wiley: New York, 1999.

KUNASZ, I. Lithium resources, Industrial minerals, and rocks, *in*: KOGEL, J. E. (ed); **Industrial minerals & rocks: commodities, markets, and uses**. Littleton, 2006.

LI, C.; XU, Y.; JIANG, X. The fractal model of mineral deposits. **Geology of Zhejiang**, 10, 1994. p.25-32 .

LIMA, A.; DE VIVO, B.; CICCHELLA, D.; CORTINI, M.; ALBANESE, S. Multifractal IDW interpolation and fractal filtering method in environmental studies: An application on regional stream sediments of (Italy), Campania region. **Applied Geochemistry**, 18, 2003. p.1853-1865.

MANDELBROT, B. B. The Fractal Geometry of Nature. **American Journal of Physics**, 51, 1983. p. 455-468.

MARVIN, R. D. **Dean Lithium project national instrument 43-101 technical report**. Cypress Development Corp.: Nicosia, 2018.

NAZARPOUR, A. Application of C-A fractal model and exploratory data analysis (EDA) to delineate geochemical anomalies in the: Takab 1:25,000 geochemical sheet, NW Iran, Iranian **Journal of Earth Sciences**, 10(2), 2018. p. 173-180.

NAZEMI, E.; ARIAN, M. A.; JAFARIAN, A.; POURKERMANI, M.; YAZDI, A. Studying The Genesis Of Igneous Rocks In Zarin-Kamar Region (Shahrood, Northeastern Iran) By Rare Earth Elements. **Revista Gênero e Direito**, 8(4): 2019. p. 446-466. DOI: https://doi.org/10.22478/ufpb.2179-7137.2019v8n4.48442

NOROUZI, M.; ABEDINI, A. Provenance and paleo-redox conditions of shales of the Shemshak Formation (Lower Jurassic) in northwest of Iran. **Thirty fifth Geological Conference**, Geological Survey of Iran: Tehran, 2017.

RAHIMI, M.; MORADZADEH, A.; ABEDI, M.; ARAB-AMIRI, A. Sequential Factor Analysis for Au Exploration in Alut 1:100,000 Sheet. **Conference, Research in Geosciences**, Tehran, 2017

SAADATI, H.; TORSHIZIAN, H. **Investigation of the relationship between the material of the stone with Lithium concentration in evaporation-alluvial rocks in the range of gypsum marls in Khorasan Razavi province**. Dissertation, Department of Geology, Islamic Azad University (North Tehran Branch), Tehran, Iran, 2012.

SADEGHI, B.; MOAREFVAND, P.; AFZAL, P.; YASREBI, A.; DANESHVAR, L. Application of fractal models to outline mineralized zones in the Zaghia iron ore deposit, Central Iran. **Journal of Geochemical Exploration**, 122, 2012. p. 9-19.

SIMMT, E.; DAVIS, B. Fractal Cards: A Space for Exploration in Geometry and Discrete Mathematics. **Mathematics Teacher**, 91, 1998. p. 102-108. <https://eric.ed.gov/?id=EJ559990>.

TENG, F. Z.; MC DONOUGH, W. F.; RUDNICK, R. L.; DALPÉ, C.; TOMASCAK, P.; CHAPPELL, B. W.; GAO, S. Lithium isotopic composition and concentration of the upper continental crust. **Geochimica et Cosmochimica Acta**, 68, 2004. p.4167-4178.

VAN-HELVOORT, P. J.; FILZMOSER, P.; VAN-GAANS, P. F. M. Sequential Factor Analysis as a new approach to multivariate analysis of heterogeneous geochemical datasets: An application to a bulk chemical characterization of fluvial deposits (Rhine–Meuse delta, The Netherlands). **Applied Geochemistry**, 20, 2005. p. 2233-2251.

YASREBI, A. B.; HEZARKHANI, A. Resources classification using fractal modelling in Eastern Kahang Cu-Mo porphyry deposit, Central Iran, **Iranian Journal of Earth Sciences**, 11(1), 2019. p. 56-67.

YAZDI, A.; SHAHHOSINI, E.; DABIRI, R.; ABEDZADEH, H. Magmatic Differentiation Evidences And Source Characteristics Using Mineral Chemistry In The Torud Intrusion (Northern Iran). **Revista Geoaraguaia**, 9(2), 2019a. p. 6-21.

YAZDI, A.; ASHJA ARDALAN, A.; EMAMI, M. H.; DABIRI, R.; FOUDAZI, M. Magmatic interactions as recorded in plagioclase phenocrysts of quaternary volcanics in SE Bam (SE Iran), **Iranian Journal of Earth Sciences**, 11(3), 2019b. p. 215-225.

YONG, A. G.; PEARCE, S. **A Beginner's Guide to Factor Analysis**: Focusing on Exploratory Factor Analysis. Tutorials in Quantitative Methods for Psychology, 9, 2013. p.79-94. <https://pdfs.semanticscholar.org/ 24e7/84058b56c4 de64f.247dec89fb7a759efa116.pdf>

YOUSEFI, M.; KAMKAR-ROHANI, A.; CARRANZA, E. J. M. Application of staged factor analysis and logistic function to create a fuzzy stream sediment geochemical evidence layer for mineral prospectivity mapping. **Geochemistry: Exploration, Environment, Analysis,** 14, 2014. p.45-58.

ZUO, R.; Decomposing of mixed pattern of arsenic using fractal model in Gangdese belt, Tibet, China. **Applied Geochemistry**, 26, 2011. p. 271-273.